

**STRUCTURAL AND ELECTROCHEMICAL STUDY OF HIGH  
VOLTAGE CATHODE MATERIAL,  $\text{Li}_2\text{MnO}_3$ , AND IT'S REDOX  
REACTION ANALYSIS**

A PROJECT REPORT

SUBMITTED IN FULFILMENT OF THE REQUIREMENTS FOR THE AWARD OF THE  
DEGREE

OF

MASTER OF SCIENCE

IN

PHYSICS

Submitted by:

**NAVEEN 2K21/MSCPHY/31**

**RITU RATHORE 2K21/MSCPHY/62**



Under the Supervision of

**Dr. AMRISH K. PANWAR**

DEPARTMENT OF APPLIED PHYSICS  
DELHI TECHNOLOGICAL UNIVERSITY

(Formerly Delhi College of Engineering)

Bawana Road, Delhi - 110042

## **CANDIDATE'S DECLARATION**

We hereby certify that the project which is presented in Dissertation – II titled “**Structural and electrochemical study of high voltage cathode material,  $\text{Li}_2\text{MnO}_3$ , and its Redox Reaction analysis**” and submitted to the Department of Applied Physics, Delhi Technological University, Delhi, is a record of our own, carried out from January to May 2023 under the supervision of Dr. Amrish K. Panwar. We have not submitted the matter presented in this report for the award of any other degree of this or any other Institute/University. The work has been communicated in a peer-reviewed Scopus-indexed conference with the following details:

**Title of the Paper (I):** Structural and electrochemical study of high voltage cathode material,  $\text{Li}_2\text{MnO}_3$ , and its Redox Reaction analysis

**Author names:** Naveen, Ritu Rathore, and Amrish K. Panwar

**Name of Conference:** International Conference on Advance Materials for Emerging Technologies

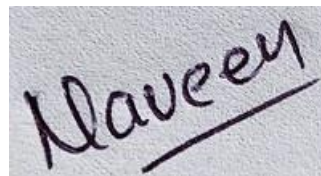
**Conference Dates with the venue:** 4<sup>th</sup>-6<sup>th</sup> May,2023, Netaji Subhas University of Technology, New Delhi – 110078 (India).

**Conference Registered (Yes/No)? :** Yes

**Status of paper (Accepted/Published/Communicated):** Accepted.

Place: Delhi

Date: 30 may,2023



**Naveen Yadav (2K21/MSCPHY/31)**



**Ritu Rathore (2K21/MSCPHY/62)**

**DELHI TECHNOLOGICAL UNIVERSITY**

**(Formerly Delhi College of Engineering)**

**Bawana Road, Delhi - 110042**

**SUPERVISOR CERTIFICATE**

To the best of my knowledge, the above work has not been submitted in part or complete for any Degree or Diploma to this University or elsewhere. I further certify that the publication and indexing information given by the students is correct.

Date: 30<sup>th</sup> May, 2023.

Place: New Delhi

Dr. Amrish K. Panwar

*Assistant Professor*

*Department of Applied Physics*

*Delhi Technological University*

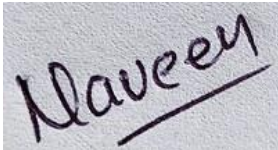
*(Formerly Delhi College of Engineering)*

*Bawana Road, Delhi - 110042*

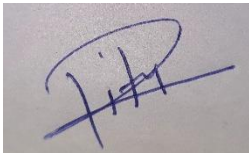
## ACKNOWLEDGEMENT

We would like to express our sincere gratitude to our guide and mentor, Dr. Amrish K. Panwar, for guiding and assisting us in every step of this project. We are extremely grateful to him for giving us clear direction and moral support to carry out the project. We would like to thanks Mr. Sharad Singh Jadaun, Ms Shivangi Rajput for their continuous help

We would also like to express our gratitude to the Dept. of Applied Physics for providing us with the required labs, infrastructure, and environment which permitted us to perform our task without any hindrance.

A handwritten signature in blue ink that reads "Naveen" with a horizontal line underneath.

**Naveen Yadav (2K21/MSCPHY/31)**

A handwritten signature in blue ink that appears to be "Ritu" with a horizontal line underneath.

**Ritu Rathore (2K21/MSCPHY/62)**

## CONTENTS

● Title Page.....	1
● Candidate's Declaration .....	2
● Certificate.....	3
● Acknowledgment.....	4
● Abstract.....	6
● List of Figures.....	7
● List of Tables.....	8
● List of Abbreviations .....	9
Chapter 1 - Introduction .....	11-17
1.1.    Batteries	
1.2.    Li-ion Batteries	
1.3.    Cathode materials for Li-ion batteries	
1.4.    Li <sub>2</sub> MnO <sub>3</sub>	
1.5.    Advantages and Disadvantages	
Chapter 2 - Synthesis Method .....	18-21
2.1.    Solid-State Synthesis	
2.2.    Ball Milling	
Chapter 3 - Experimental .....	22-23
3.1.    Synthesis of Li <sub>2</sub> MnO <sub>3</sub>	
3.2.    Preparation of cell	
Chapter 4 - Results and Discussions.....	24-34
4.1.    TGA	
4.2.    XRD	
4.3.    FTIR	
4.4.    Conductivity and Activation Energy	
4.5.    Electrochemical impedance spectroscopy	
4.6.    Cyclic voltammetry	
Chapter 5 - Conclusions.....	35

- References .....36
- Plagiarism Report .....37-38
- Conference Payment Details.....39
- Conference Certificate .....40
- Acceptance Report .....41

## ABSTRACT

Li-ion batteries have become indispensable in our modern, technology-driven world, powering a wide array of devices. As the demand for high-energy-density batteries continues to surge, there is a need to explore advanced cathode materials. In this regard,  $\text{Li}_2\text{MnO}_3$  has emerged as a highly promising contender for high-voltage ( $>4.5$  V) cathodes in Li-ion batteries.  $\text{Li}_2\text{MnO}_3$  offers several advantages over conventional cathode materials such as  $\text{LiCoO}_2$  and intercalation-type compounds. Notably,  $\text{Li}_2\text{MnO}_3$  possesses a remarkable high-voltage capability, which is crucial for achieving enhanced energy density in batteries. Furthermore, it exhibits favourable characteristics, including non-toxicity and ease of synthesis, making it an attractive alternative for Li-ion battery technology. In this study,  $\text{Li}_2\text{MnO}_3$  was synthesized using a solid-state route, enabling its detailed characterization. X-ray Diffraction (XRD) analysis was employed to investigate the crystallographic properties of the synthesized material. The obtained XRD patterns were subjected to rigorous structural analysis using the Rietveld refinement technique. By applying Scherrer's formula to the XRD peaks, the crystallite size of  $\text{Li}_2\text{MnO}_3$  was determined to be approximately 37.05 nm. To evaluate the electrochemical performance of  $\text{Li}_2\text{MnO}_3$  as a cathode material, Electrochemical Impedance Spectroscopy (EIS) and Cyclic Voltammetry (CV) analyses were performed. EIS measurements provided valuable insights into charge transfer resistance and ion diffusion behavior, while CV analysis revealed distinct high-voltage peaks around 4.5 V, accompanied by supplementary low-voltage peaks at approximately 3.7 V. These electrochemical findings affirm the potential of  $\text{Li}_2\text{MnO}_3$  as a high-voltage cathode material for Li-ion batteries. This study presents a comprehensive exploration of the synthesis, characterization, and electrochemical analysis of  $\text{Li}_2\text{MnO}_3$  as a high-voltage cathode material for Li-ion batteries. Its exceptional attributes make it a promising candidate for next-generation battery technology. Ongoing research and development efforts in this area will undoubtedly contribute to the advancement of Li-ion batteries, enabling the creation of more efficient and high-performance energy storage solutions.

## LIST OF FIGURES

Figure 1 – Historical timeframe of improvements in Li-ion batteries.

Figure 2 - Lithium in periodic table.

Figure 3 - Charging and Discharging in Li-ion battery.

Figure 4 – Structure of  $\text{Li}_2\text{MnO}_3$

Figure 5: Depicts the sample after taking it out of the ball-milling machine

Figure 6: Thermogravimetric Analysis curve for precursors

Figure 7: XRD and Rietveld refinement data of  $\text{Li}_2\text{MnO}_3$  synthesised at  $1000^\circ\text{C}$ .

Figure 8: FTIR curve for  $\text{Li}_2\text{MnO}_3$ .

Figure 9: Resistivity vs Temperature plot for  $\text{Li}_2\text{MnO}_3$ .

Figure 10: Variation in DC conductivity vs Temperature for  $\text{Li}_2\text{MnO}_3$ .

Figure 11: Electrochemical Impedance Spectroscopy for  $\text{Li}_2\text{MnO}_3$  cathode cell.

Figure 12: Cyclic Voltammetry Plot for  $\text{Li}_2\text{MnO}_3$

Figure 13: Cyclic voltammetry showing phase transformation of  $\text{Li}_2\text{MnO}_3$  over cycling



## LIST OF TABLES

Table 1: Depicts the Crystallographic details of  $\text{Li}_2\text{MnO}_3$  phase obtained from Rietveld analysis using XRD data.

Table 2: Depicts the Lattice parameters of  $\text{Li}_2\text{MnO}_3$  obtained from Rietveld refinement of XRD data

## **LIST OF ABBREVIATIONS AND SYMBOLS**

1. Li-ion - Lithium-ion
2. LMO - Lithium manganese oxide ( $\text{Li}_2\text{MnO}_3$ )
3. TGA - Thermogravimetric Analysis
4. XRD - X-Ray Diffraction
5. FTIR - Fourier Transform Infrared Spectroscopy
6. EIS - Electrochemical impedance spectroscopy
7. CV - Cyclic Voltammetry
8. TM – Transition Metal
9.  $\sigma$  - DC conductivity
10.  $\rho$  - Resistivity

# CHAPTER 1 - INTRODUCTION

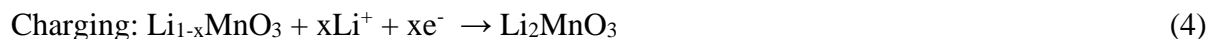
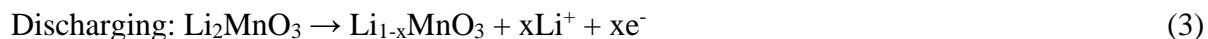
## 1.1 Batteries

A battery is used to interchange between the chemical energy into electrical energy through an electrochemical reaction. On the basis of rechargeability two kinds of battery are present: primary and secondary. In primary batteries the electrochemical reactions are irreversible hence categorized as no-rechargeable battery. In secondary batteries the reactions are reversible hence categorized as rechargeable batteries. A battery typically consists main components as the cathode, anode, electrolyte and separator. On cathode the reduction reaction takes place, accepting external circuit electrons. Conversely, an oxidation reaction occurs at the anode, donating electrons to an external circuit. The electrolyte and separator act as electronic insulators but efficient ionic conductors, allowing the movement of ions between the electrodes while preventing short-circuiting. The reactions involving in primary and secondary batteries with specific examples are shown below respectively,

For primary batteries,



For Secondary batteries,



On the historical time frame, in the 1980s the demand for outdoor audio/visual gadgets and information technology equipment like cellular phones, notebook computers, and digital cameras began to rise. Primary batteries were commonly used until the 1970s, but secondary batteries such as Ni-Cd batteries started replacing them. However, Ni-Cd batteries had limitations as power sources for portable devices, including low energy density and environmental concerns.

Sony Corporation entered the battery industry in the mid-1970s, initially focusing on primary batteries like silver oxide, carbon zinc, alkaline manganese, and primary lithium cells. As the trend shifted towards rechargeable batteries, Sony recognized the need for novel solutions. In 1985, Sony began researching secondary batteries when Ni-Cd was no longer suitable. They explored the possibility of lithium-based anodes and successfully developed the first li-ion secondary battery (LIB) in 1991.

The initial LIBs were used in cellular phones, requiring two cells connected in series due to their limited power output at the time. However, using first-generation LIBs in low ambient temperatures, such as during ski competitions, presented challenges. Extensive efforts were made to enhance LIB performance, including energy density, drain capability, cyclic performance, and discharge performance at low temperatures.

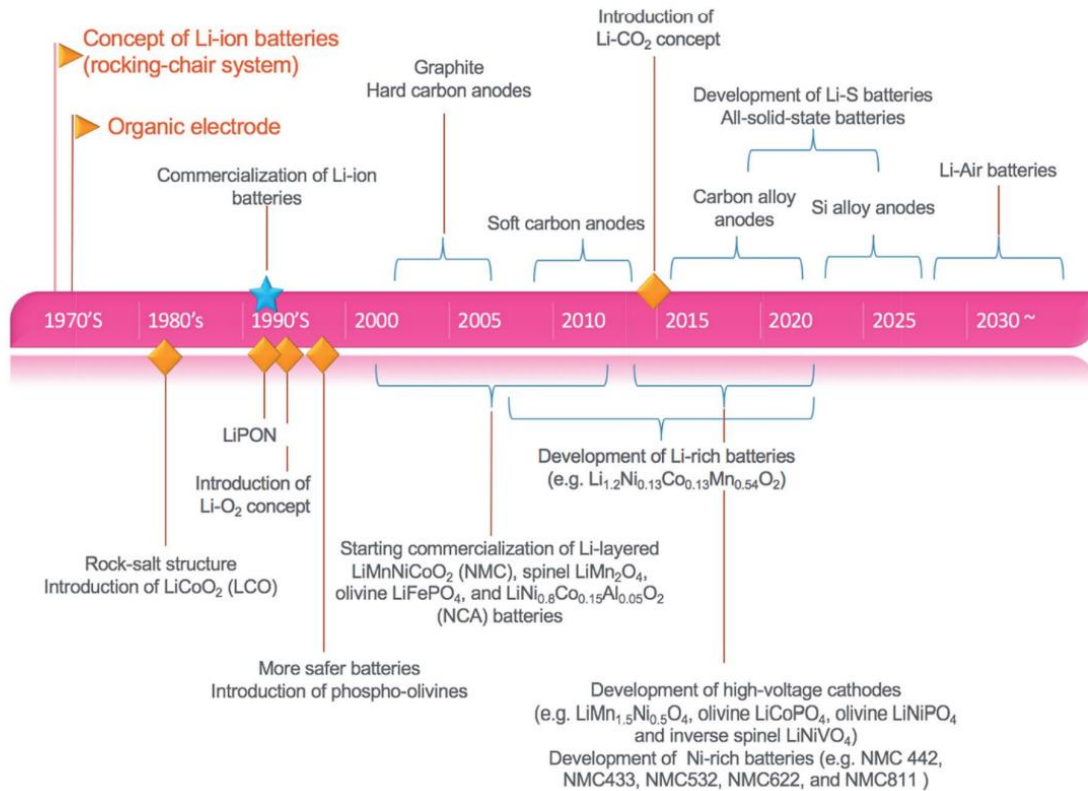


Figure 1 – Historical timeframe of improvements in Li-ion batteries. [1]

## 1.2 Lithium ion Batteries (LIB)

A lithium-ion battery, as its name implies, is a rechargeable battery that stores and releases energy by the movement of li-ions in-between the electrodes. The continuous migration of lithium ions

between these electrodes is essential for LIBs functioning. The anode, which carries a negative charge, releases lithium ions into the electrolyte. These discharged ions then travel towards the cathode, also known as the positively charged electrode, where they are absorbed. This process represents the discharge of energy in lithium-ion batteries. Likewise, during the charging process, lithium ions migrate from the cathode to the anode through the electrolyte. It is evident that the charging procedure is essentially the reverse of the discharge process.

**Why Lithium** – Lithium is the lightest metal having atomic no 3 and possesses 0.53 g/cm<sup>3</sup> density. Its remarkably low standard reduction potential (-3.05 V) makes it highly suitable for high energy density, high voltage battery cells.

1 H		
3 Li	4 Be	
11 Na	12 Mg	
19 K	20 Ca	21 Sc
37 Rb	38 Sr	39 Y

Figure 2 - Lithium in periodic table. [2]

To effectively utilize lithium, it became necessary to avoid water and air and develop non-aqueous electrolytes. The development of non-aqueous electrolytes demanded careful consideration of these factors to ensure optimal performance and safety in lithium-based batteries.

### 1.3 Working of Li-ion battery

Li intercalation and deintercalation is the main working principle of li-ion battery. During the discharge mode, oxidation occurs at the anode, causing electrons to move through the external circuit. Simultaneously, reduction occurs at cathode, by electrons from outer circuit. The potential

difference between cathode and anode determine the. During charging, the external electricity is applied to reverse the electrochemical process and stores the energy in form of chemical energy. In LIBs, the anode and cathode stores the li-ion. As the li-ions move, electrons are absorbed and emitted by electrodes giving the reversible electrochemical reactions and a current flow. The electrical current flows in outer circuit and it can be used to harness the power from LIBs.

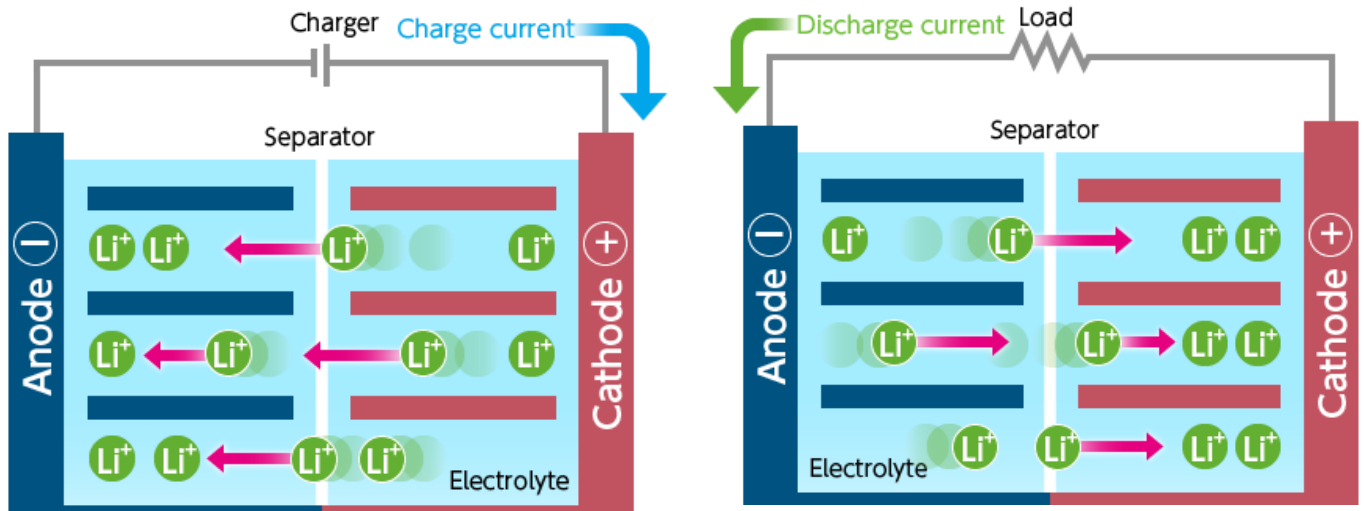


Figure 3 - Charging and Discharging in Li-ion battery. [3]

#### 1.4 Cathode Materials for li-ion battery

The active and primary source of all the Li-ions, in LIBs is cathode. There are various types of cathodes for LIBs, and still searching for new ones. Certain properties are crucial for being a suitable cathode material for LIBs:

1. It should have ions that can be reduced and oxidised easily, typically transition metal.
2. It should exhibit a reversible reaction with lithium, allowing for intercalation and deintercalation.
3. It should have high free energy when interacting with Lithium.
4. It should have high capacity, ideally allowing the Li to TM ratio be 1:1.
5. It should have high voltage i.e. around 4V to have high energy density.
6. It should have rapid reactions during insertion and removal of lithium.
7. Good electronic conductivity should be a property of cathode material as it is necessary to facilitate efficient electron transfer.

8. It should be stable, maintaining its structure and avoiding degradation under discharge and charging.
9. It should be eco-friendly and cost effective.

In rechargeable lithium-ion batteries, the mechanism of lithium intercalation and deintercalation is crucial. The cathode material's structure plays a significant role in enabling this process. Typically, cathode materials can be categorized into three main structural types as described below:

#### **Layered Structure -**

The layered cathode structure comprises stacked layers of lithium-containing TM oxides, such as lithium cobalt oxide ( $\text{LiCoO}_2$ ) and lithium manganese oxide ( $\text{Li}_2\text{MnO}_3$ ). The layers consist of transition metal atoms (e.g., Co or Mn) arranged in a close-packed oxygen lattice. Lithium ions reside in the interlayer spaces between the metal oxide layers. The transition metal atoms adopt various oxidation states to facilitate Li-ion extraction/insertion during charge/discharge. The transition metal atoms occupy octahedral coordination sites within the oxygen lattice. Lithium ions occupy interstitial sites between the metal oxide layers.

#### **Spinel Structure -**

The spinel cathode structure utilizes materials like lithium manganese oxide ( $\text{LiMn}_2\text{O}_4$ ). It consists of a face-centered cubic lattice of O-ions. Transition metal (e.g., Mn or Fe) and lithium ions occupy tetrahedral and octahedral sites within the lattice, respectively.

#### **Olivine Structure -**

The olivine cathode structure employs lithium iron phosphate ( $\text{LiFePO}_4$ ) as the active material. The olivine structure features a three-dimensional framework of corner-sharing  $\text{PO}_4$  tetrahedra. Lithium and iron ions occupy interstitial sites within this framework. Lithium ions reside in interstitial sites between the  $\text{PO}_4$  tetrahedra. Iron ions occupy octahedral coordination sites.

## 1.4 $\text{Li}_2\text{MnO}_3$

$\text{Li}_2\text{MnO}_3$  is a member of the oxide materials family and exhibits a monoclinic - C2/m space group symmetry [4]. It possesses ( $\text{A}_2\text{BO}_3$ ) type configuration represented as  $\text{Li}[\text{Li}_{1/3}\text{Mn}_{2/3}]\text{O}_2$ , where li-ions layers alternate with Mn-ion layers, with cubic-close packed oxygen planes in between them. This layered structure resembles the ideal arrangement found in  $\text{LiCoO}_2$ . The inclusion Li in the TM layer gives a higher theoretical capacity of 460 mAh g<sup>-1</sup>, making it an alternative LIB cathode. Researchers have shown a good interest in it due to ability to provide high voltage (>4.5V) [5,6,7,8,9].

In crystal structure, li-ions exists between  $\text{MnO}_6$  octahedral layers. These lithium ions are surrounded by oxygen atoms, while the manganese ions reside within the  $\text{MnO}_6$  octahedral structural. Each Mn-ion is surrounded by 6 O-atoms. O-ions act as bridge between the TM and Li layers. facilitating the coordination of both lithium and manganese ions

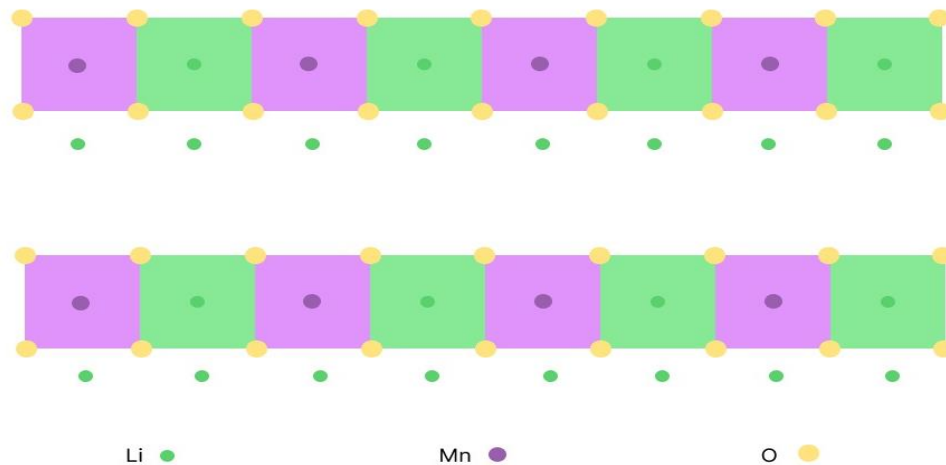


Figure 4 – Structure of  $\text{Li}_2\text{MnO}_3$

$\text{Li}_2\text{MnO}_3$  offers the advantage of a high operating voltage, allowing for increased energy density in battery systems. However, one drawback is the electrochemical inactivity of the Mn ions in their +4 oxidation state. This issue can be overcome by extraction of Li and oxygen from the structure using chemical methods. Additionally, electrochemical activation can be done by subjecting it to a voltage more than 4.5 V. During this, a phase transformation occurs, due to electrochemical reactions, resulting in the transformation its structure from layered to spinel [9,10,11]



## **1.5 ADVANTAGES and DISADVANTAGES**

### **Advantages-**

- LIBs are lightweight compared to other rechargeable battery types of the same size. This is due to the use of lightweight materials such as lithium and carbon in the electrodes.
- The atomic bonds in lithium are highly reactive, allowing for a high energy density in LIBs. They can store a significant amount of energy per unit weight compared to other batteries. For example, LIBs can store electrical energy around 150 Wh/kg.
- LIBs have a lower self-discharging, around 5% charge in a month.
- They do not suffer from memory effect, so there is no need to fully discharge them before recharging.
- LIBs are capable of operating over hundreds of cycles with good capacity retention.

### **Disadvantages-**

- LIBs have a limited lifespan typically lasting only two to three years regardless of usage.
- High temperatures can significantly accelerate the degradation of lithium-ion batteries.
- Complete discharge of a li
- Lithium-ion battery can render it unusable.
- Although rare, there is a small risk of a lithium-ion battery pack malfunctioning and causing a fire.

## CHAPTER 2 - SYNTHESIS METHODS

Synthesis of cathode material of Li-ion batteries can be done using various synthesis routes available to us. Like: -

- Solid state reaction
- sol-gel synthesis
- hydrothermal synthesis
- and many others.

In this project, we have used solid-state synthesis as our route to obtain the desired material.

### 2.1 Solid-State Synthesis

SSR involves inducing a chemical reaction between starting materials, in this case solid to produce another solid material with a well-defined structure. Several factors have to be considered when we need to select starting materials for this method. Precursors influence some very important aspects of the reaction as feasibility and reaction rate. Additionally, the reaction conditions play a significant role, parameters such as reaction temperature, calcination time, pressure, and the reaction atmosphere determine the type, and composition of the end product. The reaction atmosphere can be inert, oxidizing, or reducing, and often dictates the composition of the final product. Ultimately, the product which is the most thermodynamically stable under the given parameters will be formed. Solid-state synthesis offers a versatile approach to tailor materials with desired properties by controlling the composition, crystal structure, and morphology through careful selection of starting materials and reaction conditions. It enables the synthesis of a wide range of functional materials used in various technological applications. In laboratory settings, small porcelain crucibles are commonly used. The heating and cooling time required for the reaction can vary significantly depending on the specific reaction. Some reactions may be completed within a few hours, while others can go on for a week or so. The pressure of the reaction happening inside also needs to be adjusted accordingly. When conducting new reactions using this method, calculations and references of similar reactions in a literature are often relied upon. However, optimizing the reaction conditions for the desired outcome typically involves a degree of trial and error. Overall, the solid-state synthesis method offers flexibility in controlling reaction

parameters and allows for producing a wide range of materials with tailored properties. It is a practical approach in materials research and development, enabling the synthesis of advanced materials for various applications.

### **Procedure**

In the solid-state synthesis process, the first step involves weighing the dried starting materials in the desired quantities. These materials are then ground together using tools such as a mortar and pestle for small quantities or a ball mill for larger amounts. To provide additional help so that of the materials are mixed properly, a small amount of a solvent like acetone or ethanol can be used. This creates a slurry that transforms into a solid mixture after the solvent evaporates. Sometimes, the ground powder mixture, with help of palletizer is converted into a pellet. This compaction increases the contact area between the materials, facilitating diffusion and enhancing the reaction rate. The resulting mixture is then placed into a container which is chemically inert and can withstand very high temperature.

### **Advantages**

- Solid-state reactions are very inexpensive and it is the simplest and a very common method of sintering materials. As no expensive equipment is needed, precursors and energy usage of heating are the main cause of the cost.
- Finding solid reactants for reactions is generally not challenging, as most of them remain stable under normal conditions. There is a wide variety of oxygen or carbonate compounds available, which can be utilized in solid-state reactions.
- This method is applicable both in industrial settings and laboratory environments. It enables the synthesis of many diverse range of materials, including but not limited to mixed metal oxides, nitrides, aluminosilicates, and various other compounds.

### **Drawbacks:**

The primary challenge associated with the solid-state reaction method is the diffusion process within solid materials. Despite efforts to enhance reaction efficiency by grinding and compressing materials into pellets, the limited diffusion of molecules between different materials in solid form remains a significant bottleneck. Consequently, these reactions often require prolonged durations and high temperatures. Additionally, monitoring the ongoing reaction can be a complex task.

## 2.2 Ball Milling

In the ball mill impact from balls and attrition with particles of material is the basic principle of operation. The main idea behind its functioning is to create a collision between the fast-moving balls and the powder material inside the mill. During operation, the hollow cylinder rotates on its longitudinal axis, facilitating the attrition mode. This rotation occurs at a low speed, allowing the balls to roll over each other. This collision leads to the breakage and reduction in the size of the powder particles.

It's important to note that the ball mill operates at low speeds to prevent excessive heating and ensure efficient grinding. By carefully controlling the movement and interaction of the balls with the powder material, the ball mill serves as a versatile tool for various applications in industries such as mining, pharmaceuticals, and materials synthesis.

Ball milling relies on a cylindrical mill chamber that houses durable balls made of materials like tungsten, silicon carbide, or hardened steel. These rigid balls are set in motion within the chamber, effectively facilitating the milling process. By subjecting the initial powder material to the action of these rotating balls, the particles are reduced to nanoscale dimensions.

To initiate the ball milling process, the feed material is introduced into the cylinder in an amount that occupies approximately 60% of the cylinder's volume. A fixed number of balls is added to the mixture, and the cylinder is sealed before the mill starts its rotation. The speed at which the mill rotates is a crucial factor.

The ball mill finds its application in various uses, including

1. Fine grinding: It is effective in achieving particle sizes of 100-5 micro-meters or even smaller, making it suitable for fine grinding applications.
2. Hard and abrasive materials: The ball mill is particularly useful for processing hard and abrasive materials due to the presence of durable grinding balls that can withstand demanding conditions.

The combination of these advantages positions ball mills as versatile and valuable tools across various industries.

There are certain disadvantages associated with the use of ball mills, including:

1. Noisy operation: Ball mills can generate significant noise during operation, which can be a drawback in certain working environments.

2. Slow process: The ball milling process can be relatively slow compared to other milling methods, which may limit its suitability for applications requiring rapid processing.
3. Limitations on material types: Soft, tacky, and fibrous materials may not be suitable for milling using ball mills as they can get stuck to the balls or the inner wall of the cylinder, leading to ineffective milling or equipment damage.

## CHAPTER 3 –EXPERIMENTAL

### 3.1 Synthesis

The lithium-rich Lithium Manganese Oxide ( $\text{Li}_2\text{MnO}_3$ ) was synthesized via solid-state route. A stoichiometric amount of Lithium Carbonate ( $\text{Li}_2\text{CO}_3$ ) (m.w.=73.89 g/mol, purity=98.5%) was used as a source of lithium. Manganese Oxide( $\text{MnO}$ ) (m.w.=70.94g/mol, purity=99%) was used as a source for manganese.

The precursors were weighed and then ball milled. For the milling process, we used stainless steel jar and balls. The ball milling process was run for 24 hours with a rest time of half hour after a fixed interval of half hour giving the effective time for milling as 12 hours. The rotation was clockwise and it was the same for the whole milling process. The ball milling is done in an ethanol medium. The rotation per minute for the ball miller was set at 350 rpm. Thermogravimetric analysis was done to the well mixed precursors to analyse its decomposition and calcination temperature. The homogeneously mixed precursors were then calcined at  $1000^\circ\text{C}$  for 12 hours in an air atmosphere (determined by performing TGA).



Figure 5: Depicts the sample after taking it out of the ball-milling machine

The synthesized and well-ground powdered sample is prepared for the pallet formation by a pelletizer. Pallets of diameter 13mm were prepared. The pellet was then sintered at  $800^\circ\text{C}$  for 4h.

### **3.2 Cell Manufacturing**

The half-cell was assembled using synthesized  $\text{Li}_2\text{MnO}_3$  as an active material for the cathode with the anode being used as lithium metal foil. The slurry is prepared by making a solution for cathode with a weight percentage of the active material as 80%, 10% weight percentage of conductive carbon, and 10% weight percentage of the binder. Due to the universal solvent nature of NMP, it was used to prepare a slurry of the above combination by magnetic stirring for 10h at  $50^\circ\text{C}$  temperature. The prepared slurry of the above composition was applied on the substrate of aluminium foil of thickness 20 microns by using a doctor's blade. It was then placed in a vacuum oven is used to dry for 12h at  $80^\circ\text{C}$ .

The coin cell was assembled in a glove box with control of moisture and oxygen. Li-foil is used as an anode, polypropylene porous membrane as a separator membrane and,  $\text{LiPF}_6$  as an electrolyte. The coin cell is assembled in an argon atmosphere inside the glove box. The open circuit voltage after assembling and settling for 24h is observed around 2.7V as the  $\text{Li}_2\text{MnO}_3$  is not activated yet.

## CHAPTER 4 - RESULTS AND DISCUSSIONS

### 4.1 Thermogravimetric Analysis

The main objective of thermal analysis is to establish the relationship between temperature and specific physical and chemical properties of materials. Thermo-galvanometric analysis was done by using Perkin Elmer TGA 4000 to analyse the decomposition of the precursors in the N<sub>2</sub> environment due to its chemically inert nature. The TGA analysis is operated up to 800°C with an increase in 10°C temperature per minute, choosing N<sub>2</sub> gas as an inert atmosphere. The thermal behaviour is shown in Figure 6.

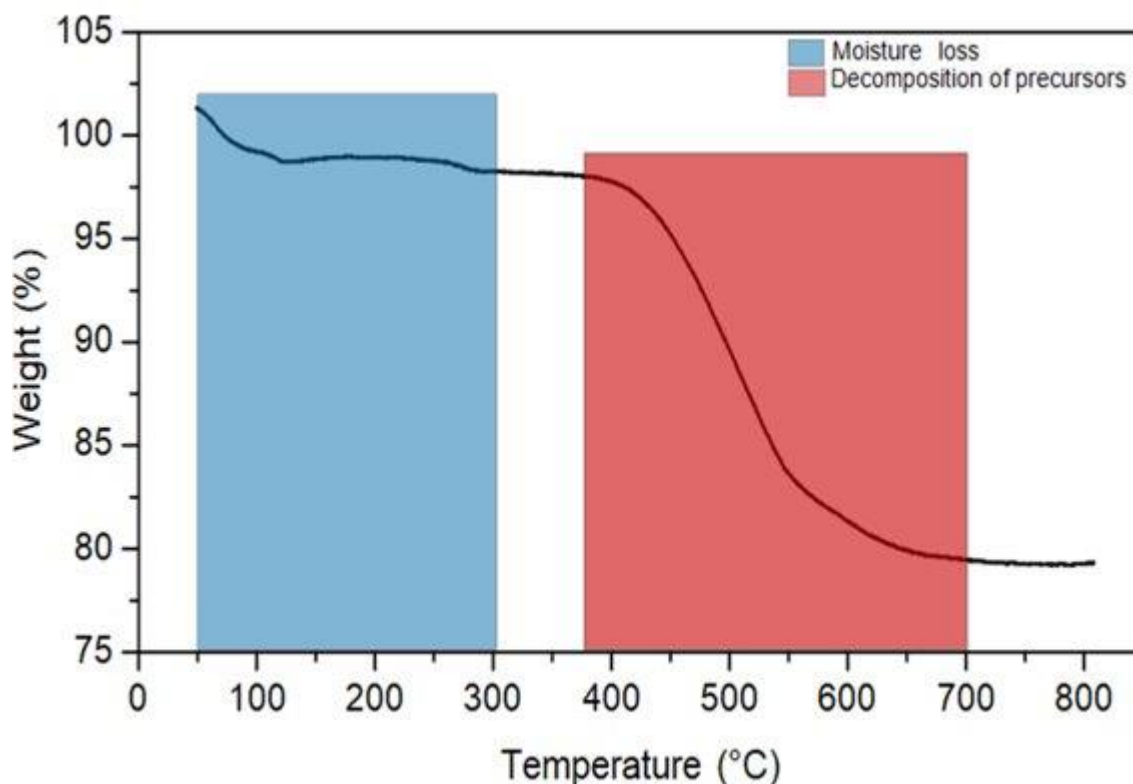


Figure 6: Thermogravimetric Analysis curve for precursors

There were two phases in which the weight reduction is observed. The first weight loss is from 50°C to 300°C, it is due to moisture and other volatile impurities. The second weight loss occurs from 400°C to 700°C, it is due to the decarburization due to the decomposition of precursors and



the release of CO<sub>2</sub> gas. After 700°C, there was no variation in weight is observed that indicates the thermodynamically stable Li<sub>2</sub>MnO<sub>3</sub> formation, as reported previously [10].

## 4.2 X-Ray Diffraction

XRD is a non-destructive technique used to analyse the crystallographic structure of a material. By exposing a crystalline material to an X-ray beam, diffraction patterns are generated, providing valuable insights into its structural and crystalline properties. By utilizing this approach, essential characteristics of materials can be determined, including the arrangement of atoms in the crystal lattice, the extent of crystalline order, the dimensions of individual crystalline units, the distance between atoms, identification of specific crystal phases, and the occurrence of phase changes along with their respective ratios. The diffraction of the radiation from the sample, happens only at angles that obey Bragg's Law(6)

$$n\lambda = 2d\sin\theta \quad (1)$$

Where,

n denotes integer (1, 2, 3, 4, ..),

d<sub>hkl</sub> = the interplanar spacing between the planes,

θ = incident angle at which X-Ray falls on the sample.

The X-Ray Diffraction spectroscopy is carried out on BRUKER D8 ADVANCE with CuKα wavelength 1.54Å in the 2theta range from 15° to 75° as the major peaks lie in this region. The peak position at 2theta values of 18.698°, 37.044°, 44.573°, 44.796°, 64.5°, 65.579° are indexed as (001), (130), (-202), (131), (-133), (-331) planes by confirming with the International Diffraction Data Card. So, the crystalline monoclinic C2/m structure is confirmed as Li<sub>2</sub>MnO<sub>3</sub>. The analysis of crystallographic details of the synthesized Li<sub>2</sub>MnO<sub>3</sub> is done using X-ray diffraction

(XRD) and Rietveld refinement of the XRD data [4,9]. The X-Ray Diffraction pattern refined using Rietveld is shown in Figure 7.

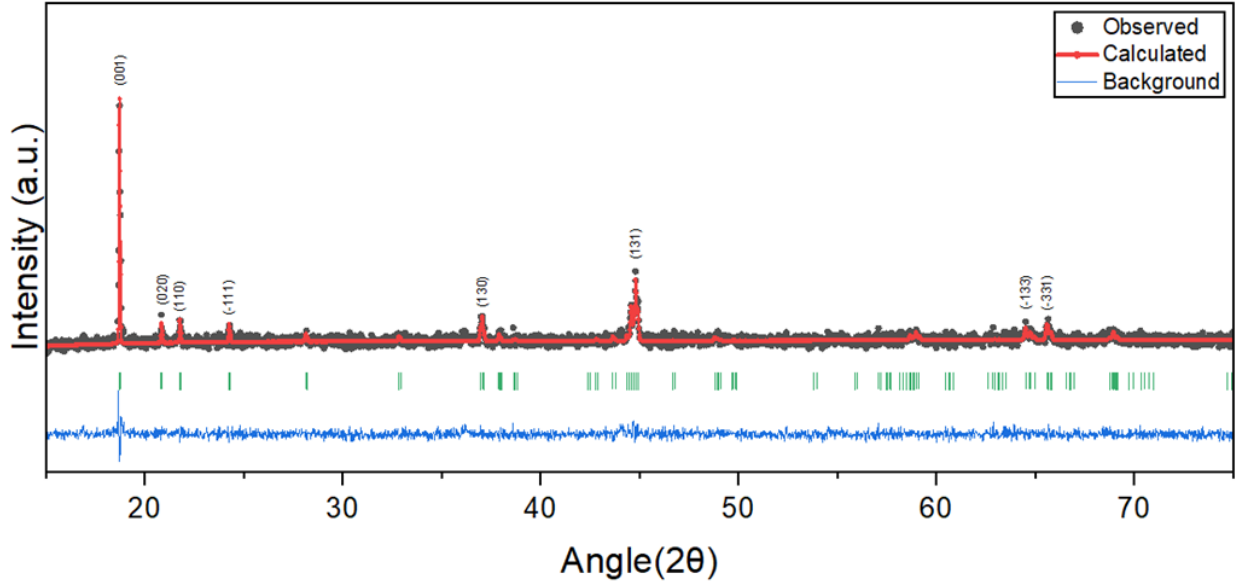


Figure 7: XRD and Rietveld refinement data of  $\text{Li}_2\text{MnO}_3$  synthesised at  $1000^\circ\text{C}$ .

Table 1: Crystallographic details of  $\text{Li}_2\text{MnO}_3$  phase obtained from Rietveld analysis using XRD data:

Particle	site	X	Y	z
Li-1	2b	00.0000	0.5000	0.0000
Li-2	2c	0.0000	0.0000	0.5000
Li-3	4h	0.0000	0.70390	0.5000
Mn-1	4g	0.0000	0.17267	0.0000
O-1	4i	0.23910	0.0000	0.20094
O-2	8j	0.21897	0.34886	0.22440

Table 2: Lattice parameters of  $\text{Li}_2\text{MnO}_3$  obtained from Rietveld refinement of XRD data

Crystal Structure	a	b	c	$\alpha$	$\beta$	$\gamma$	Cell Volume
Monoclinic C2/m	4.9288	8.5262	5.0274	90	109.409	90	199.2644

The goodness of the fit in Rietveld refinement is 1.158 with Bragg-R factor = 31.7,  $\text{ATZ} = 420.585$ ,  $R_p = 157$ ,  $R_{wp} = 66.1$ . The prominent peak at  $2\theta = 18.7^\circ$  i.e. (001), corresponds to  $\text{Li}_2\text{MnO}_3$  and other unit cell parameters are in good coordination with previously reported studies. The high peak intensities and Rietveld refinement of XRD data support the high crystallinity of the synthesised material.

### 4.3 Fourier Transform Infrared Spectroscopy (FTIR)

FTIR is a non-destructive characterization technique which we use for determining the molecular bonds in compounds and functional groups presented in sample. IR absorption bands in the spectrum as wave numbers is used to identify the chemical components undetectable by XRD. FTIR spectroscopy offers a high degree of sensitivity, capable of detecting even trace amounts of substances in a sample [7]. The FTIR spectra for as-prepared  $\text{Li}_2\text{MnO}_3$  are shown in Figure 8.

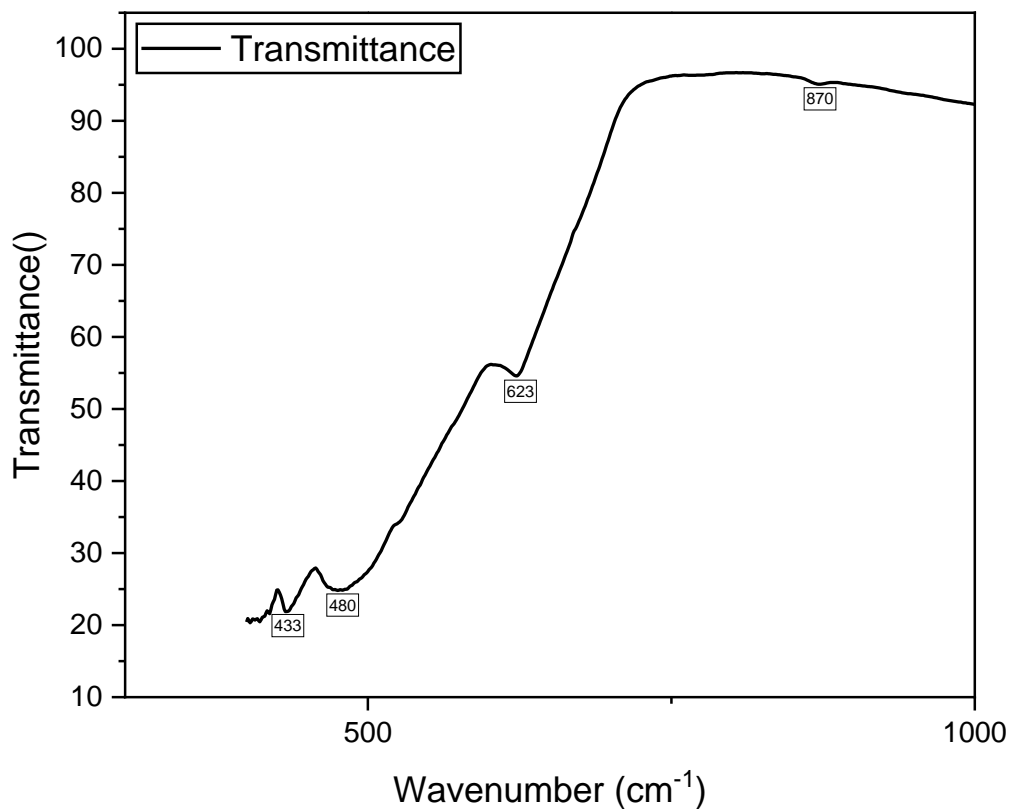


Figure 8: FTIR curve for Li<sub>2</sub>MnO<sub>3</sub>.

The frequency band at 420 – 650 cm<sup>-1</sup>, indicates the li and Mn in octahedral coordination. The frequency band around 870 cm<sup>-1</sup> is for the -OH peaks from the KBr disks as they can be observed in the absence of Li<sub>2</sub>MnO<sub>3</sub>

#### 4.4 CONDUCTIVITY AND ACTIVATION ENERGY ANALYSIS

Electrical conductivity reflects the ease with which a material allows electrical current to flow through it. On the other hand, electrical resistivity tells us how strongly a material resists the flow of electrical current .

The pellet prepared earlier is then used to analyse the DC conductivity. The pellet is placed perfectly in the probe setup in the Source Measurement Unit. Then the resistance, voltage, current, and resistivity is measured with varying temperature in two-phase – The heating Phase and the

Cooling Phase. The setup is prepared to raise the temperature to 200 °C and then cooled down to 40°C.

The graph between Resistivity and Temperature is shown in Figure 6.

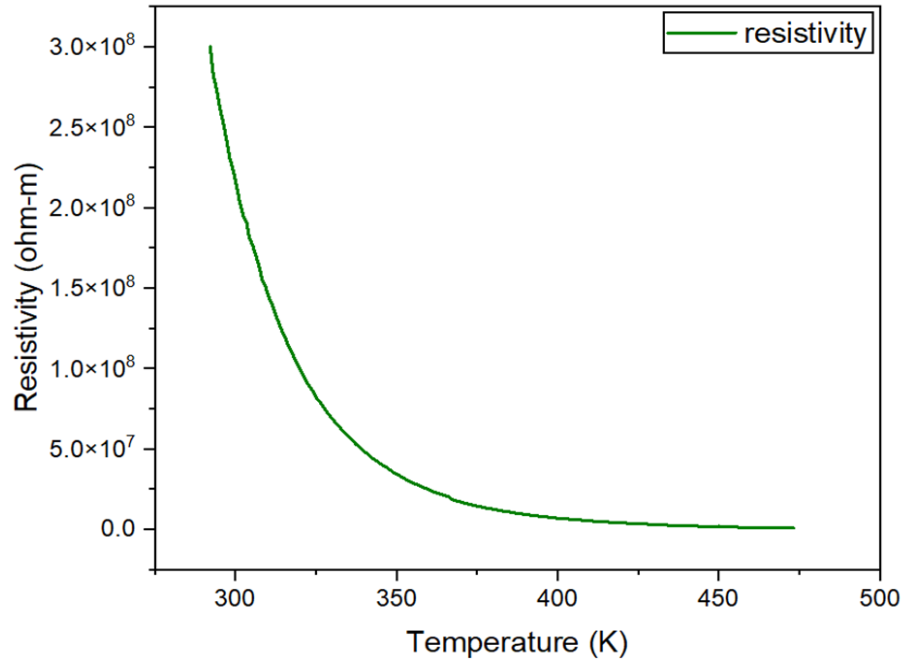


Figure 6: Resistivity vs Temperature plot for Li<sub>2</sub>MnO<sub>3</sub>.

The DC conductivity is calculated by the relation between resistivity and conductivity being inverse of each other, as:

$$\sigma = \frac{1}{\rho} \quad (5)$$

Where,  $\sigma$  = DC conductivity

$\rho$  = Resistivity.

The DC conductivity is calculated as **2.63\*10<sup>-7</sup> S/cm**.

The graph between the log of conductivity vs  $1000/T$  is shown in the figure 7.

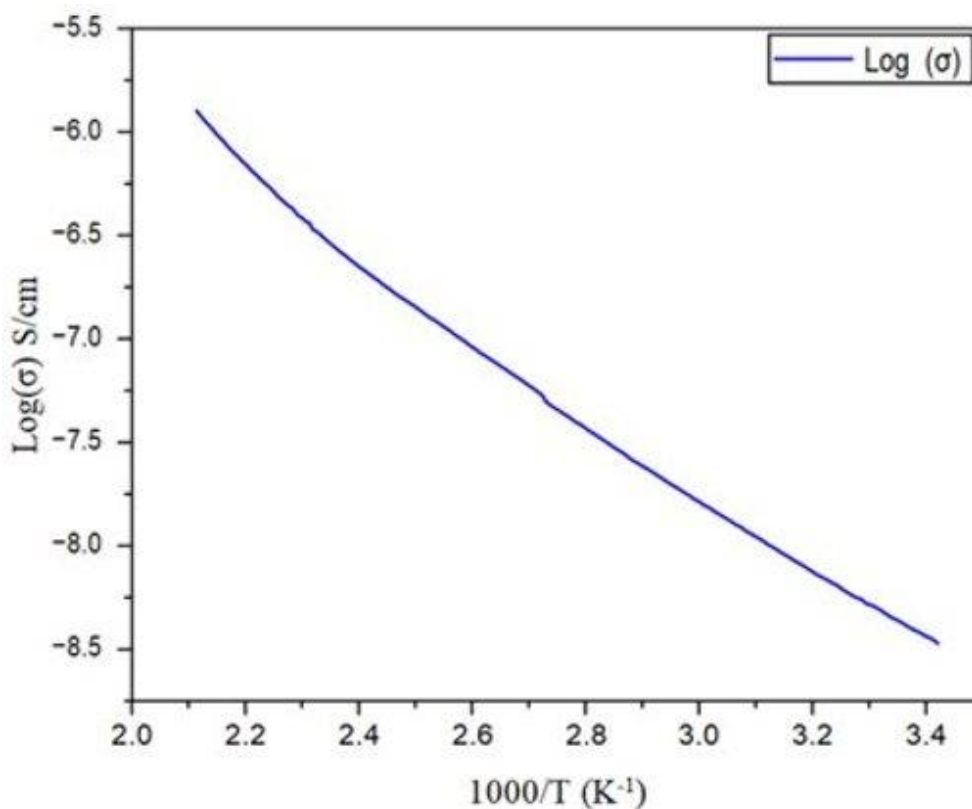


Figure 7: Variation in DC conductivity vs Temperature for  $\text{Li}_2\text{MnO}_3$ .

The activation energy for pristine  $\text{Li}_2\text{MnO}_3$  is calculated using the Arrhenius equation which Comes as  $E_a = 1.56\text{eV}$ .

#### 4.5 ELECTROCHEMICAL IMPEDANCE SPECTROSCOPY

EIS is an important experimental technique providing valuable insights into electrochemical systems. EIS offers the advantage of measuring a broad range of frequencies, enabling the examination of internal processes with varying time constants. While Ohm's law describes a linear decrease in cell voltage when neglecting internal processes, the actual voltage decline occurs in three distinct stages. The first stage involves ohmic losses, which occur immediately after the current pulse without any time delay. The second phase involves voltage reductions resulting from charge transfer, occurring delayed, by the double-layer capacity. The third phase involves voltage decreases due to li-ions diffusion into the active material, persisting until the voltage drop reaches its conclusion.

In the EIS technique, a cell is subjected to a sinusoidal signal, and the subsequent unique response is captured and studied. This response is dependent on the cell's impedance. Hence, this is the basic principle of EIS. The galvanostatic or potentiostatic parameters can be used as Current and Voltage respectively.

The assembled cell was characterized by electrochemical impedance spectroscopy in frequency range 10mHz to 100KHz. The cell impedance is observed as 356 ohms.

The Nyquist plot for EIS is shown in the figure 8.

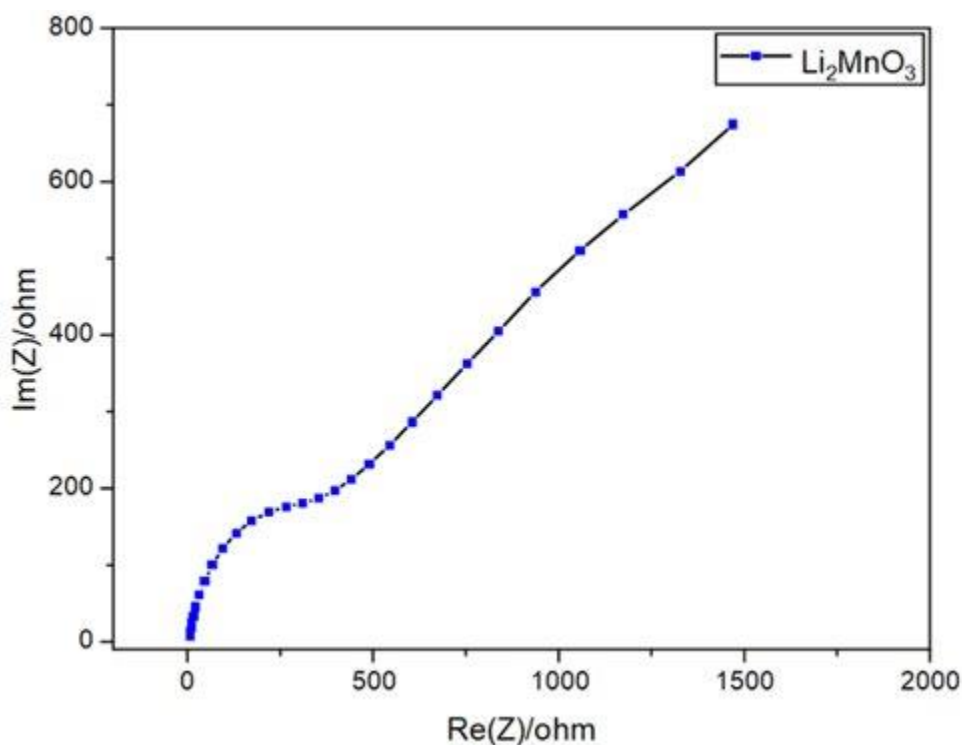


Figure 8: Electrochemical Impedance Spectroscopy for  $\text{Li}_2\text{MnO}_3$  cathode cell.

#### 4.6 CYCLIC VOLTAMMETRY

Cyclic voltammetry is a technique derived from linear sweep voltammetry, which involves measuring the current as the potential is linearly varied with respect to time. The rate at which we change the voltage over time is called as the scan rate ( $\text{m s}^{-1}$ ). Within CV measurements, the scan rate ( $v$ ) serves as a crucial parameter. The voltage is swept from  $E_1$  to  $E_2$ , representing gradient of a linear voltage change throughout the measurement. We can get very useful information about voltage and cyclability of the reactions occurring by conducting multiple cycles under identical

conditions. Also, it can be used to investigate the kinetics of electrochemical redox reaction by changing the scan rate.

CV analysis was performed to analyse and understand the intercalation/deintercalation mechanism of the electrochemical reaction of lithium in  $\text{Li}_2\text{MnO}_3$  cell at scan rate 0.5 mV/s with voltage varying between 2.5V to 4.7V . The CV curve of  $\text{Li}_2\text{MnO}_3$  is shown in Figure 9.

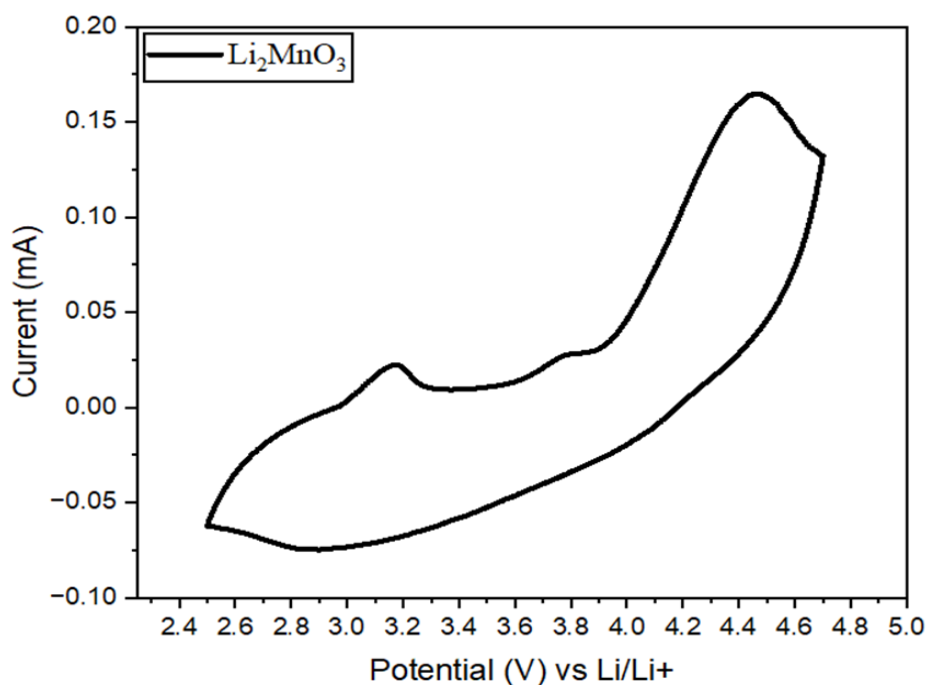


Figure 9: Cyclic Voltammetry Plot for  $\text{Li}_2\text{MnO}_3$ .

The CV curve shows two peaks at approx. 3.7V and 4.5V for charging and a steep slope for discharging. First peak around 3.7V and second peak at 4.5V indicates the removal of li-ions from Li layer and Transition metal layer, respectively. This electrochemical behaviour is because of the unique crystallographic structure of  $\text{Li}_2\text{MnO}_3$ . In the unit cell of the crystal there are 4 atoms of Li, at positions being 1 at the corner and crystallographic faces were occupied by the remaining three Li atoms, as reported previously. At the lower voltages the Li ion present at the surface of the unit cell are extracted and the Li ions inside the cell requires high voltage, giving rise to the two-phase lithium extraction process and the splitting of the peaks in CV [11,12,13,14].

The peak at high voltage around 4.5V is irreversible in nature because the extraction of Li at this voltage rises structural changes in the material. The CV curve for first four cycles is shown in figure 10.



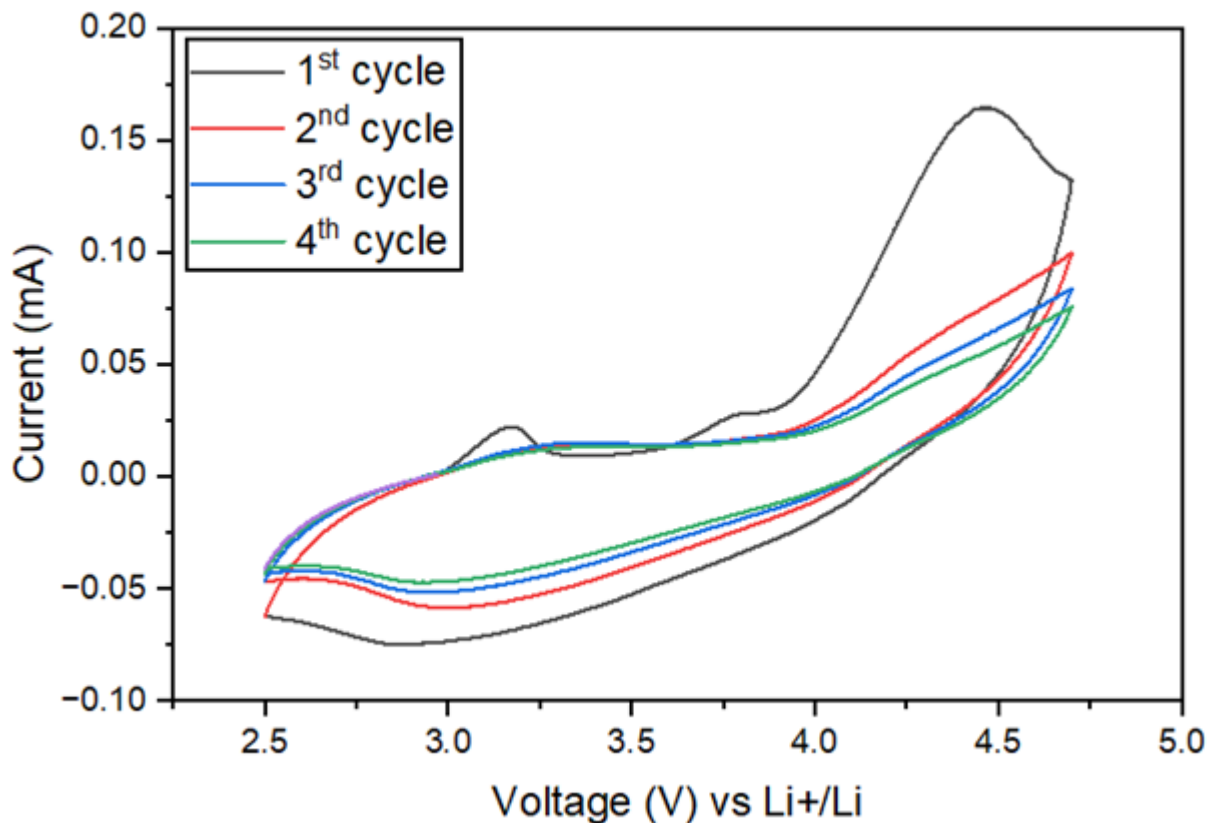


Figure 10: Cyclic voltammetry showing phase transformation of  $\text{Li}_2\text{MnO}_3$  over cycling.

The plateau around 4.5V disappears over cycling, along with this the peak around 3V is developed with cycling indicating the Spinal Phase formation from  $\text{Li}_2\text{MnO}_3$ , it is because of the 2-phase extraction or delithiation process in  $\text{Li}_2\text{MnO}_3$  and it could also indicate the electrolyte oxidation as reported by Alastair D. Robertson and Peter G. Bruce, that the delithiation and intercalation occurs in  $\text{Li}_2\text{MnO}_3$  in two ways, one being the Li-ion replaced with  $\text{H}^+$  ions, another being the oxygen ion removal giving the charge balance during delithiation and with no experimental observation of Mn dissolution or disproportion indicates the oxidation of electrolyte at electrode surface giving the exchange of  $\text{H}^+$  ions with  $\text{Li}^+$  ions [12,13].

As in  $\text{Li}_2\text{MnO}_3$ , the oxidation state of Mn atom is 4+, the further oxidation of Mn in the octahedral region is reported to be impossible in  $\text{Li}_2\text{MnO}_3$ . So there can be anionic redox activity (involvement of O in redox reaction) in  $\text{Li}_2\text{MnO}_3$  during the delithiation and intercalation, this is reported by many authors based on the experimental observation of shortening of interplanar

distances of O-O by synchrotron diffraction. It can also be explained by the relation of Fermi Level to the electrochemical redox potential i.e. electron below fermi level and holes above fermi level. The band structure of  $\text{Li}_2\text{MnO}_3$  consist orbital overlap of d-orbital of Mn and three p-orbitals of Oxygen atom resulting in M-O bonding and anti-bonding bands. In cationic redox the non-bonding M-O bands are involved in redox process. For lithium manganese oxides, the theoretical reports explain the  $\text{O}_2$  consisting one 2s and three 2p doublets with non-involvement of 2s in redox reaction because it lies in the deep energy and participation of higher energy doublets in M-O bonding. But in case of  $\text{Li}_2\text{MnO}_3$  like structures having higher O/Mn ratio, one of the three 2p doublets of O i.e. the one closer to Li atom, is bonded weakly in M-O bonding due to its small overlapping the 2s orbitals of Li. This behaves like the non-bonding state of O lying above the stabilized bonding of M-O giving rise to two band redox process as the electrons can also be removed from the 2p non-bonding bands of oxygen giving it an extra capacity. As with a good cooperation of experimental observations in this work, the two peaks in CV curves during charging is reported that in case of  $\text{Li}_2\text{MnO}_3$ , the redox process involves M-O non-bonding bands and also the 2p non-bonding bands of oxygen.

The Capacity fading in  $\text{Li}_2\text{MnO}_3$  can be explained by the irreversible removal of  $\text{O}_2$ , transition metal occupying the  $\text{Li}^+$  sites after delithiation, phase transformation from layered to spinal with formation of  $\text{MnO}_2$  like phase and generation of anionic and cationic vacancies giving rise to structural transformation and capacity fading as reported previously.

## CHAPTER 5 - CONCLUSION

The pristine  $\text{Li}_2\text{MnO}_3$  was synthesised by solid state route and analysed that it has good crystallinity using XRD and FTIR analysis and crystallite size is observed as 37.05nm. The Electrochemical Characterization is done using EIS analysis and CV analysis. The cell impedance is observed to be 356 ohm. Peak splitting in CV curve is observed at 3.7V and 4.5V. This is explained and understood by the anionic redox mechanism, charge balance, electrolyte oxidation and decomposition.

## REFERENCES

- 1 Mehek, R. *et al.* (2021) 'Metal–organic framework-based electrode materials for lithium-ion batteries: A Review', *RSC Advances*, 11(47), pp. 29247–29266. doi:10.1039/d1ra05073g.
- 2 Sbade (2019) *Chemie-Nobelpreis: „sie schufen eine Wiederaufladbare Welt" - sonnenseite - ökologische kommunikation mit Franz Alt, Sonnenseite*. Available at: <https://www.sonnenseite.com/de/wissenschaft/chemie-nobelpreis-sie-schufen-eine-wiederaufladbare-welt/> (Accessed: 30 May 2023)
- 3 Ray, A.K. *et al.* (2022) 'Comparison between ultra-high-temperature thermal battery and Li-Ion Battery', *Lecture Notes in Mechanical Engineering*, pp. 469–481. doi:10.1007/978-981-19-3379-0\_39.
4. Wang LB, Hu HS, Lin W, Xu QH, Gong JD, Chai WK, et al. Electrochemically Inert Li<sub>2</sub>MnO<sub>3</sub>: The Key to Improving the Cycling Stability of Li-Rich Manganese Oxide Used in Lithium-Ion Batteries. *Materials*. 2021 Aug 23;14(16):4751.
5. Gu M, Belharouak I, Zheng J, Wu H, Xiao J, Genc A, et al. Formation of the Spinel Phase in the Layered Composite Cathode Used in Li-Ion Batteries. *ACS Nano*. 2013 Jan 22;7(1):760–7.
6. Assat G, Tarascon JM. Fundamental understanding and practical challenges of anionic redox activity in Li-ion batteries. *Nat Energy*. 2018 Apr 9;3(5):373–86.
7. Robertson AD, Bruce PG. Mechanism of Electrochemical Activity in Li<sub>2</sub>MnO<sub>3</sub>. *Chemistry of Materials*. 2003 May 1;15(10):1984–92.
8. Wang R, He X, He L, Wang F, Xiao R, Gu L, et al. Atomic Structure of Li<sub>2</sub>MnO<sub>3</sub> after Partial Delithiation and Re-Lithiation. *Adv Energy Mater*. 2013 Oct;3(10):1358–67.
9. Boulineau A, Croguennec L, Delmas C, Weill F. Structure of Li<sub>2</sub>MnO<sub>3</sub> with different degrees of defects. *Solid State Ion*. 2010 Jan 29;180(40):1652–9.
10. Strobel P, Lambert-Andron B. Crystallographic and magnetic structure of Li<sub>2</sub>MnO<sub>3</sub>. *J Solid State Chem*. 1988 Jul;75(1):90–8.
11. Lu W, Wu Q, Dees DW. Electrochemical Characterization of Lithium and Manganese Rich Composite Material for Lithium Ion Batteries. *J Electrochem Soc*. 2013 Apr 16;160(6):A950–4.
12. Chennakrishnan S, Thangamuthu V, Subramaniam A, Venkatachalam V, Venugopal M, Marudhan R. Synthesis and characterization of Li<sub>2</sub>MnO<sub>3</sub> nanoparticles using sol-gel technique for lithium ion battery. *Materials Science-Poland*. 2020 Jun 1;38(2):312–9.
13. Kalyani P, Chitra S, Mohan T, Gopukumar S. Lithium metal rechargeable cells using Li<sub>2</sub>MnO<sub>3</sub> as the positive electrode. *J Power Sources*. 1999 Jul;80(1–2):103–6.
14. Yu DYW, Yanagida K, Kato Y, Nakamura H. Electrochemical Activities in Li<sub>2</sub>MnO<sub>3</sub>. *J Electrochem Soc*. 2009;156(6):A417.

# Plagiarism Report



Similarity Report ID: oid:27535:36512073

PAPER NAME

**for plag thesis-1.docx**

WORD COUNT

**4991 Words**

CHARACTER COUNT

**27439 Characters**

PAGE COUNT

**24 Pages**

FILE SIZE

**1.5MB**

SUBMISSION DATE

**May 30, 2023 5:03 PM GMT+5:30**

REPORT DATE

**May 30, 2023 5:04 PM GMT+5:30**

## ● 3% Overall Similarity

The combined total of all matches, including overlapping sources, for each database.

- 1% Internet database
- Crossref database
- 2% Submitted Works database
- 0% Publications database
- Crossref Posted Content database

## ● Excluded from Similarity Report

- Bibliographic material
- Cited material
- Quoted material
- Small Matches (Less than 10 words)

**● 3% Overall Similarity**

Top sources found in the following databases:

- 1% Internet database
- 0% Publications database
- Crossref database
- Crossref Posted Content database
- 2% Submitted Works database

## TOP SOURCES

The sources with the highest number of matches within the submission. Overlapping sources will not be displayed.

1	<b>Hunter Valley Grammar School on 2020-11-29</b> Submitted works	<1%
2	<b>Sungkyunkwan University on 2019-11-01</b> Submitted works	<1%
3	<b>Imperial College of Science, Technology and Medicine on 2008-06-02</b> Submitted works	<1%
4	<b>Chulalongkorn University on 2019-12-10</b> Submitted works	<1%
5	<b>Indian Institute of Technology, Kanpur on 2016-05-02</b> Submitted works	<1%
6	<b>Song, Liubin, Zhaohui Tang, Yang Chen, Zhongliang Xiao, Lingjun Li, Ho...</b> Crossref	<1%
7	<b>University of Birmingham on 2017-03-27</b> Submitted works	<1%
8	<b>library.unisel.edu.my</b> Internet	<1%

Sources overview

## Conference Payment Details

**paytm**

Money Sent Successfully

**₹2,000** 

Rupees Two Thousand Only



DBTR/311519255815/25-04-2023 09:02:24/  
UPI

To: Bank Account



From: Naveen

Paytm Bank - 9718



UPI Ref No: 311519255815

09:02 AM, 25 Apr 2023

POWERED BY  
**UPI**  
UNIFIED PAYMENTS INTERFACE

## Conference Certificate



*Department of Physics*  
Netaji Subhas University of Technology  
Sec-3, Dwarka, New Delhi-110078, India

### *Certificate of Presentation*

This certificate is proudly awarded to Prof./Dr./Mr./Ms. Naveen  
from DTU, New Delhi

Paper Title: Structural and electrochemical . . . . . Reaction analysis

For your excellent oral/ poster presentation at the conference and your significant contribution to the success of **International Conference on Advanced Materials for Emerging Technologies (ICAMET- 2023)**, held during **May 4-6, 2023**, at Netaji Subhas University of Technology, New Delhi - 110078, India.

  
**Dr. Anurag Gaur**  
Convener



  
**Prof. Ranjana Jha**  
Conference Chair



# ACCEPTANCE REPORT



Amrish kumar panwar <amrish.phy@dtu.ac.in>

---

## regarding your paper presented in ICAMET 2023

1 message

---

International Conference <icamet@nsut.ac.in>  
To: amrish.phy@dtu.ac.in

Tue, May 30, 2023 at 1:28 PM

Dear Prof. Panwar, Greetings!

Your paper entitled “Structural and electrochemical study of high voltage cathode material,  $\text{Li}_2\text{MnO}_3$ , and its Redox Reaction analysis” presented by Naveen et al in ICAMET 2023 has been accepted after the internal review process for publication in the Conference proceedings published by Royal Book Publishing-Eleyon Publishers, Tamil Nādu, India. The formatting and other details in this regard will be communicated later.

Thank you for presenting your work in ICAMET-2023.

Organising Committee  
ICAMET-2023